

In Silico Study and Validation of Phosphotransacetylase (PTA) as a Putative Drug Target for *Staphylococcus aureus* by Homology-Based Modelling and Virtual Screening

V. K. Morya · Varun Dewaker · Eun-Ki Kim

Received: 29 April 2012 / Accepted: 4 September 2012 /
Published online: 6 October 2012
© Springer Science+Business Media, LLC 2012

Abstract *Staphylococcus aureus*, a Gram-positive bacterium, can cause a range of illnesses from minor skin infections to life-threatening diseases, such as bacteraemia, endocarditis, meningitis, osteomyelitis, pneumonia, toxic shock syndrome and sepsis. Due to the emergence of antibiotic resistance strains, there is a need to develop of new class of antibiotics or drug for this pathogen. The phosphotransacetylase enzyme plays an important role in the acetate metabolism and found to be essential for the survival of the *S. aureus*. This enzyme was evaluated as a putative drug target for *S. aureus* by in silico analysis. The 3D structure of the phosphotransacetylase from *S. aureus* was modelled, using the 1TD9 chain 'A' from *Bacillus subtilis* as a template at the resolution of 2.75 Å. The generated model has been validated by PROCHECK, WHAT IF and SuperPose. The docking was performed by the Molegro virtual docker using the ZINC database generated ligand library. The ligand library was generated within the limitation of the Lipinski rule of five. Based on the dock-score, five molecules have been subjected to ADME/TOX analysis and subjected for pharmacophore model generation. The zinc IDs of the potential inhibitors are ZINC08442078, ZINC8442200, ZINC 8442087 and ZINC 8442184 and found to be pharmacologically active antagonist of phosphotransacetylase. The molecules were evaluated as non-carcinogenic and persistent molecule by START programme.

Keywords Phosphotransacetylase (PTA) · *S. aureus* · Homology modelling · Molecular docking · Pharmacophore

Introduction

Staphylococcus aureus causes a variety of suppurative (pus-forming) infections and toxinoses in humans. It causes superficial skin lesions such as boils, styes and furuncles; more serious

V. K. Morya (✉) · V. Dewaker · E.-K. Kim
National Research Laboratory of Bioactive Materials, Department of Biological Engineering,
Inha University, Incheon 42-751, Korea
e-mail: moryavvie@gmail.com

E.-K. Kim
e-mail: ekkim@inha.ac.kr

infections such as pneumonia, mastitis, phlebitis, meningitis and urinary tract infections; and deep-seated infections, such as osteomyelitis and endocarditis [1–5]. *S. aureus* is a major cause of hospital-acquired (nosocomial) infection of surgical wounds and infections associated with indwelling medical devices [1, 3, 4]. *S. aureus* causes food poisoning by releasing enterotoxins into food and toxic shock syndrome by release of super-antigens into the blood stream [6, 7]. *S. aureus* has been identified with various kinds of virulence factors, which are biochemical properties that enhance their survival (carotenoids and catalase production); surface proteins, promoting colonisation of host tissues; invasins (hyaluronidase, kinases and leukocidin); surface factors (capsule and protein A); immunological disguises (protein A and coagulase); membrane-damaging toxins (haemolysins, leukotoxin and leukocidin); exotoxins (SEA-G, TSST and ET); and inherent and acquired resistance to antimicrobial agents, [8–13]. Targeting these number of virulence factors to design any antibiotic is not an easy task. The rate of emergence of antibiotic resistance strain of *S. aureus* is so horrible that about 90 % are resistant against penicillin while 50 % strains are multidrug resistant; thus, the battle remains [3, 14]. Targeting any molecule is not just sufficient to develop effective antimicrobials. The computational approach has been used to investigate novel drug targets in other pathogenic organisms, such as *Pseudomonas aeruginosa* [15, 16], *Mycoplasma genitalium* [17], *Aspergillus* [18, 19, 53] and *Helicobacter pylori* [15, 20]. As most currently known, antibacterial are essentially inhibitors of certain bacterial enzymes; any bacteria-specific enzyme could be considered as potential drug targets [5, 18, 19, 21].

In our previous work, we have done a comparative metabolic pathway analysis to find out some potential targets against *S. aureus* [5]. Enzymes, which were found to be unique in compare to host proteome, have been investigated further for their drugability properties. Thus, in present study, we have evaluated the phosphotransacetylase (PTA) as a putative target. PTA (EC: 2.3.1.8) is a 328-amino-acid-containing enzyme, encoded by the *etuD* gene, also known as phosphate acetyltransferase, phosphotransacetylase and phosphoacetylase [22, 23]. This enzyme is involved in three different pathways, namely, taurine and hypotaurine metabolism, pyruvate metabolism and propanoate metabolism (KEGG database). The acetyl-co-A or acetate, an intermediary compound, plays a very important role in the fulfilment of energy requirement process [5, 24]. PTA is capable to cleave the short chain CoA esters besides acetyl-CoA, such as propionyl-CoA and butyryl-CoA, but is unable to hydrolyse either the succinyl-CoA or the long-chain fatty acyl CoA, palmityl-CoA [25]. Many anaerobic/fermentative/facultative/methanogenic microbes using them by specific pathways are capable of converting the acetyl-CoA to acetate by the action of phosphotransacetylase, and acetate kinase is used for the production of ATP, which provides the majority of the energy. Although the main work is involved in the acetate metabolism, acetate is an end product of almost all anaerobic/fermentative/facultative/methanogenic microbes and in turn serves as a growth substrate [26, 27]. Thus, inhibition of PTA could effectively inhibit growth and propagation of *S. aureus*. To date, no structural or drug-targeting information against the *S. aureus* using PTA has become available.

In this study, we present structural information on the PTA, which may be a novel drug target for studies aimed at developing inhibitors of *S. aureus*—using a homology modelling approach followed by a molecular dynamics simulation in order to analyse the stability of this domain. In addition, we predict the binding site of this PTA in order to eventually identify drug-like molecules that possess enhanced binding energies and pharmacokinetic properties for this enzyme using in silico high-throughput virtual screening with acetyl phosphate (DB02897) as a reference ligand. The potential specific drug-like molecules obtained from such a screening procedure could serve as inhibitors against the *S. aureus*.

Materials and Method

Sequence Retrieval, Physicochemical Characterisation and Secondary Structure Prediction

The sequences of PTA from *S. aureus* were retrieved from protein database available on NCBI server. The physicochemical properties of PTA, like theoretical isoelectric point (pI), molecular weight, total number of positive and negative residues, extinction coefficient [28], instability index [29], aliphatic index [30] and grand average hydropathy (GRAVY) [31], were evaluated by ExPASy's ProtParam server [32]. SOPMA [33] was employed for calculating the secondary structural features of the phosphotransacetylase sequences used in this study.

Cellular Localisation and Functional Elucidation

The sub-cellular localisation analysis of this essential protein has been done by Proteome Analyst Specialized Sub-cellular Localization Server v2.5 (PA-SUB) [34]. For prediction of "S-S" bonds from the primary structure (protein sequence data), the CYS_REC (<http://sun1.softberry.com/berry.phtml?topic>) was used. The domains and family of protein were confirmed by the Prosite database [35].

Homology Modelling

A 328-amino-acid-containing phosphotransacetylase sequence of *S. aureus* N315 was retrieved from NCBI database and identified with gi|15926266| and accession NP_373799. The FASTA file of the sequence was submitted to EsysPred3D, a server for prediction of proteins 3D structure based on the homology modelling [36]. An alignment-based predicted model was obtained by above server. The available model and secondary structure was validated by the STRIDE [37]. Energy minimisation and root mean square deviation (RMSD) was performed by YASARA and SuperPose servers, respectively [38, 39]. The RMSD analysis of the developed model was evaluated by means of deviation from its template using SuperPose. The SuperPose web server rapidly and robustly calculates both pairwise and multiple protein structure superposition using a modified quaternion eigenvalue approaches [39]. This modelled structure was submitted to UCLA and PROCHEK server to ensure the quality and stereochemistry of generated structure [19, 40]. The information of active site PTA used in this study was not found in the CSA database [41] and was not archived with the active site of the PTA used in this study.

Preparation of Ligand Library

The acetyl phosphate (DB 02897), a known inhibitor for the PTA, was retrieved from drug bank database, and the initial values of this molecule was used for the library generation [5]. The ligand library was prepared from ZINC database using the parameters $-1.5 \leq xlogP \leq 5$, $2 \leq H \text{ donors} \leq 5$, $5 \leq H \text{ acceptors} \leq 10$, $140.03 \leq \text{molecular weight} \leq 500$ under the limit of the Lipinski rule of five [42, 51, 52].

Docking

The virtual docking study of our predicted 3D model of phosphotransacetylase with the library prepared was performed with the molecular docking algorithm MolDock [5, 19, 43]

using the Molegro Virtual Docker version 1.1.1 software (Molegro ApS, Aarhus, Denmark, <http://www.molegro.com>) according to instructions. The docking procedure consisted of three interrelated components: (a) identification of binding site, (b) a search algorithm to effectively sample the search space (the set of possible ligand positions and conformations on the protein surface) and (c) a scoring function or energy calculation software [42, 54]. For docking, the MolDock scoring function, which is based on a piecewise linear potential and a re-ranking procedure was applied to the highest ranked poses to increase docking accuracy, was used. Ligands modelled in Arguslab and protein structure complexes were imported into the docking programme assigning bonds, hybridisation and explicit hydrogen if missing and always charges and flexible torsions with the Molegro Virtual Docker software. The molecular structure of imported ligands was manually checked before docking and corrected in those cases where it had failed. Although our structure only contains proteins, neither co-factor nor ligands are present. Water molecules with the protein structures were excluded from the docking experiments [54–56]. The default setting of software parameter was used in this study, and ligands are given from our library prepared in mol2 format. Binding sites were restricted within a $15 \times 15 \times 15 \text{ \AA}^3$ cube centered at the observed binding of ligand in protein complex. Due to the stochastic nature of the ligand–protein docking search algorithm, 10 runs were conducted and 10 docking solutions (pose) were retained for each ligand. The interaction energy between the pose with highest ranking MolDock score and the protein was compared [54–56].

Pharmacophore Generation and Tox Studies

Alignment and hypothetical pharmacophore model generation was done by Ligandscout 2.03 [44]. Ligandscout offers a large range of chemical feature definitions including hydrogen bonding vectors, chargeable groups, aromatic plane interactions and aromatic-positive ionisable interactions. An advanced alignment algorithm allows to overlay pharmacophore and molecules such that common binding modes may be detected and shared chemical features can be interpolated, and tox studies is done using the commercially available software toxtree (developed by Ideacon Ltd, Sofia, Bulgaria) for the computer-based estimation methods in the assessment of chemical toxicity [45].

Results and Discussion

The selection of phosphotransacetylase (EC: 2.3.1.8) for present study is a result of our previous study, in which we have extensively analysed the pathways of *S. aureus*, for the search of essential enzyme. This enzyme was found to be essential. This enzyme has no similarity with human proteins when search with BLASTp. This 238-amino-acid-containing enzyme is a product of eutD gene. The phosphotransacetylase as one of the essential for survival of microbe could be a putative drug target for design and evaluation of new class of antimicrobials [5, 18, 19].

Physicochemical and Functional Properties of Phosphotransacetylase

Parameters computed using ExPASy's ProtParam tool are represented in Table 1. The calculated pI (isoelectric point) of the phosphotransacetylase is 4.72, i.e. ($pI < 7$), which means that the protein is acidic in nature. The extinction coefficient of the protein is required to establish a quantitative study of protein–protein, and protein–ligand interaction in the

Table 1 Physiochemical and functional properties of phosphotransacetylase

Analysis	Parameters and respective properties									
Physiochemical properties	MW	pI	-R	+R	EC	II	AI	GRAV		
	34,951.7	4.72	45	32	10,555	34.61	98.17	Y 0.086		
Calculated secondary structure (by SOPMA)	Alpha helix,	3 ₁₀ helix,	Pi helix,	Beta bridge,	Extended strand,	Beta turn,	Bend region,	Random coil,	Ambiguous states,	
	46.95 %	0.00 %	0.00 %	0.00 %	14.02 %	7.93 %	0.00 %	31.10 %	0.00 %	
CYS_REC, PA-SUB and SOSUI analysis	CYS_REC: C167 and C310			PA-SUB: CYTOPLASM			SOSUI: SOLUBLE PROTEIN			

solution was elucidated as $10,555 \text{ M}^{-1} \text{ cm}^{-1}$. Instability index of this enzyme was calculated as 34.61 because the value is lower than 40; thus, it is a stable protein [29]. The aliphatic index (AI), which is defined as the relative volume of a protein occupied by aliphatic side chains (A, V, I and L), is regarded as a positive factor for the increase in thermal stability of globular proteins, and the calculated value was found to be 98.17. The GRAVY value for a peptide or protein is calculated as the sum of hydropathy values of all the amino acids, divided by the number of residues in the sequence. GRAVY indices of phosphotransacetylase were found to be 0.086 (Table 1). This low range of value indicates the possibility of better interaction with water. The enzyme has been analysed by SOSUI and found to be a soluble cytoplasmic protein. It is well known that disulphide bridges play a vital role for the thermal stability of the protein; the probable disulphide bond deduced by the CYS_REC is provided in Table 1. There is no any positive prediction revealed by this analysis. We have not found any pattern, motif, signature or fingerprint when the sequence was submitted to Prosite server. The secondary structure of protein was predicted by the self-optimised prediction method with alignment (SOPMA), which correctly predicts 69.5 % of amino acids for a state description of the secondary structure prediction [33]. Secondary structure features as predicted by SOPMA is represented in Table 1.

Homology Modelling and Docking

The 3D structure of the enzyme phosphotransacetylase from *S. aureus* was modelled by EsysPred3D, an automated homology modelling server (Fig. 1). Alignments are obtained by combining, weighting and screening the results of several multiple alignment programmes, and the final structure was built using the modelling package MODELLER [36]. The template used for the present investigation was 1TD9 chain 'A' from *Bacillus subtilis*, which was used for 3D structure modelling; the resolution was 2.75 Å, analysed by X-ray diffraction [25]. The server result shows that this template shares 64.4 % identities with our query sequence (using ALIGN programme, shown in Fig. 2), while BLASTp result against PDB database shows 99 % query coverage. PTA shares high sequence similarity with the reported bacterial and the archaeal domain PTAs (BLAST search results, data not shown).

The structural properties of phosphotransacetylase from the *M. thermophilla* shows that cys159 is required for the stability and possibly catalysis and cys312 as being present in the active site, but non-essential for catalysis; the residues arg87, arg133 and arg 310 were proposed to interact with CoA [27, 46]. The phosphotransacetylase from *S. aureus* shows

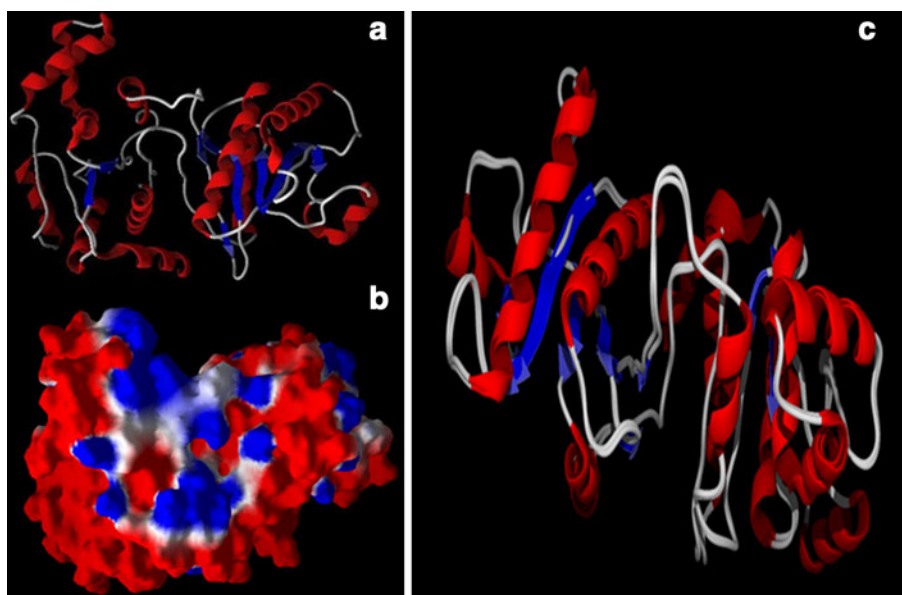


Fig. 1 Predicted 3D structure of phosphotransacetylase. **a** Secondary structure representation. **b** Surface representation. **c** Superposition of the predicted structure with template (PDB access code: 1TD9)

cys167 and cys310 and arg88, arg 89, arg134, arg148, arg285 and arg308 residues; here, it is anticipated that arg88, arg134 and arg308 and cys167 and cys310 may be involved in the active site. To validate the hypothesis of active site predicted for PTA, the CSA server was used; unfortunately, there was no nay archive with EC: 2.3.1.8 [41]. The alignment study shows that the residues cys167 and cys310 and arg88, arg 89, arg134, arg148, arg285 and arg308 could be involved in active site formation. The secondary structure of the PTA was

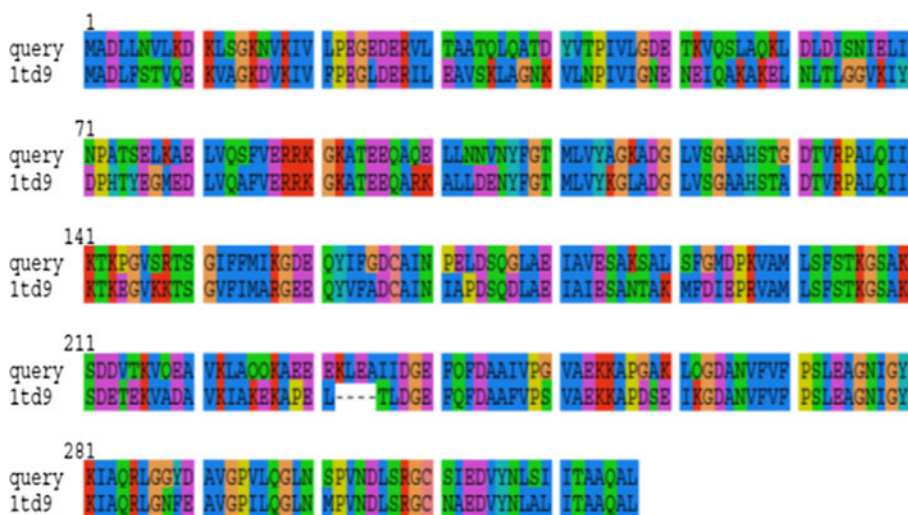


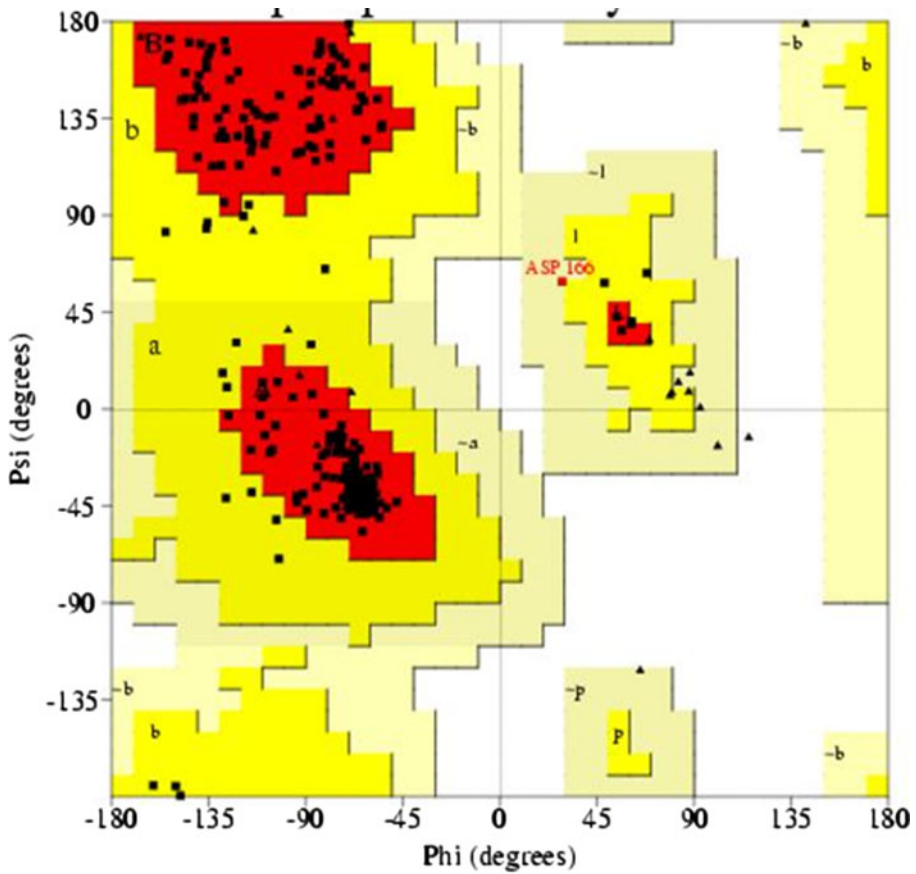
Fig. 2 Sequence alignment of phosphotransacetylase from *staphylococcus aureus* n315 with Cain A (PDB access code: ltd9) from *Bacillus subtilis*

elucidated by STRIDE [37] to analyse the pattern. The modelled structure was subjected for the force field energy minimisation, and final value was $-176,747.6$ kJ/mol, and the score is shown to be -0.09 compared to the initial values of $-56,133.5$ kJ/mol and -2.97 , respectively. The $C\alpha$ RMSD and the backbone RMSD deviations for the model and the template crystal structure were found to be 0.64 and 0.65 Å, respectively. During the compact structure comparison, the amount of native secondary structure is not so good a measure of progress towards the native free energy basin as the number of native contacts [47]. Therefore, the other parameter was studied to evaluate the quality of predicted structure. The Ramachandran plot for the predicted model reveals that 92.3% residues were found in most favourable region, while 7.6% were found in the allowed region (Fig. 3). The overall G factor calculated on basis of the main chain parameter inferred that the modelled structure was acceptable for virtual screening [48].

Docking of ligands of generated library with modelled structure of the enzyme was performed using the MolDock algorithm [43]. Recent developments in molecular characterisation and bioinformatics have further made it possible to “dock” small molecules (i.e. ligands) towards proteins and “score” their potential binding. Virtual screening uses computational methodologies to identify biologically active molecules against a specific protein target [49]. Here, we had used the methodology that involved the search for similarity to validated ligands and molecular docking method, using the crystallographic data of the targets. Nevertheless, very limited information on PTA from *S. aureus*, and their respective inhibitors is yet available. The novelty of the present study relays on the method used in virtual screening and the selection of molecules according to pharmacological properties. The virtual screening was performed with a modelled structure, which qualifies the required condition for being a suitable model for docking. Thus, methods like docking and virtual screening are becoming widely used in drug development. Thus, selection of a valid Dock protocol based on similarity of all re-docked poses to the crystallographically identified bound orientations was a major concern during the experimental. The symmetry corrected RMSD was computed for all poses. Virtual screening is one of the fastest methods employed in the drug discovery process, which is used to filter the undesired molecules, which cannot show the affinity to the proteins active site. Here, we keep our attention to the Lipinski rules, one of the criteria to filter the molecule, which cannot show the drug-like property. The docking was performed with a library of 1,001 molecules, generated under mentioned conditions. Based on dock score, five ligands were selected using two search algorithms in conjugation with two scoring functions per poses returned. It was found that the cavity 1 was involved in binding to most of ligands, having a volume of 48.128 Å³ and a surface area of 148.48 Å², respectively. Under these circumstances, the docking was performed to estimate the interaction energy between the ligand and protein. Thus, the MolDock score and hydrogen bond energy of each ligand were the primary criteria for selecting the molecules. The properties of the selected compounds like H-bond donor, H-bond acceptor, molecular weight, molecular formula, *xlogp*, compound ID, zinc ID, ligand name, etc. are shown in Table 2. We have chosen these ligands based on their docking score. The top 5 selected ligand molecules and their binding position at the cavity are shown in Fig. 4. The residue involved in the formation of cavity is also shown in Fig. 5a and the hydrogen bond interaction at the near cavity residue with the ligand molecule in Fig. 5b.

ADME/Toxtree Prediction and Phamacophore Model Generation

After docking simulation, based on MolDock score, the top 25 compound were selected from the initial set of 1,001 molecules. These molecules were submitted to filter for its

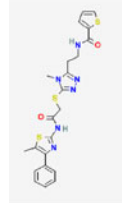
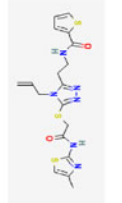
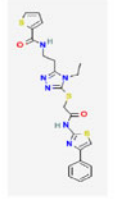
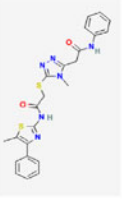
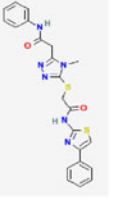


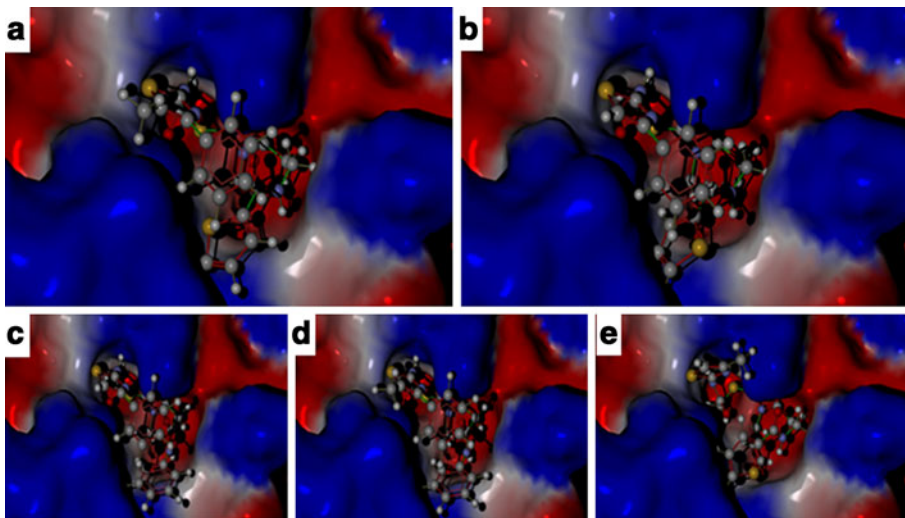
	A	P	Ctv	Cbw	Mbw	
Ramachandran plot quality	286	92.3	83.8	100	0.9	Inside
Residues (A,B,L)						
Peptide bond planarity	326	6.0	6.0	3.0	0.0	Inside
Bad non-bonded interactions	0	0.0	4.2	10.0	-0.4	Inside
Calpha tetrahedral distortion	300	1.5	3.1	1.6	-1.0	Inside
Main-chain hydrogen bond energy	211	0.7	0.8	0.2	-0.7	Inside
Overall G-factor	327	0.2	-0.4	0.3	1.9	better

A: Amino acids involved; P: Parameter value; Ctv: comparison of typical value; Cbw: Comparison value of band worth; Mbw: No. Of band widths from mean

Fig. 3 Ramachandran plot of phosphotransacetylase from *Staphylococcus aureus* obtained by PROCHECK: 92.3 % residues in favourable regions; 7.3 % residues in additional allowed regions; 0.3 % residues in generously allowed regions; 0.0 % residues in disallowed regions

Table 2 Physicochemical properties of the five selected ligands obtained from the docking study

	Ligand molecule				
Properties	ZINC8442078	ZINC 8442200	ZINC 8442087	ZINC 8442184	ZINC 8442182
					
Compound ID:	9542913	9542940	9542914	3660145	4612017
Molecular Weight	498.64408	448.5854	498.64408	478.58978	464.5632
Molecular Formula	C ₂₂ H ₂₂ N ₆ O ₂ S ₃	C ₁₈ H ₂₀ N ₆ O ₂ S ₃	C ₂₂ H ₂₂ N ₆ O ₂ S ₃	C ₂₂ H ₂₂ N ₆ O ₂ S ₂	C ₂₂ H ₂₀ N ₆ O ₂ S ₂
XLogP3-AA	3.9	3	3.8	3.4	3
H-Bond Donor	2	2	2	2	2
H-Bond acceptor:	5	5	5	5	5
IUPACName	N-[2-[4-methyl-5-[2-[(5-methyl-4-phenyl-1,3-thiazol-2-yl)amino]-2-oxoethyl]sulfanyl-1,2,4-triazol-3-yl]ethyl]thiophene-2-carboxamide	N-[2-[5-[2-[(4-methyl-1,3-thiazol-2-yl)amino]-2-oxoethyl]sulfanyl-4-prop-2-enyl-1,2,4-triazol-3-yl]ethyl]thiophene-2-carboxamide	N-[2-[4-ethyl-5-[2-oxo-2-[(4-phenyl-1,3-thiazol-2-yl)amino]ethyl]sulfanyl-1,2,4-triazol-3-yl]ethyl]thiophene-2-carboxamide	2-[4-methyl-5-[2-[(5-methyl-4-phenyl-1,3-thiazol-2-yl)amino]-2-oxoethyl]sulfanyl-1,2,4-triazol-3-yl]-N-phenylacetamide	2-[4-methyl-5-[2-oxo-2-[(4-phenyl-1,3-thiazol-2-yl)amino]ethyl]sulfanyl-1,2,4-triazol-3-yl]-N-phenylacetamide
Docking score: -	-188.8	-181.242	-180.403	-179.924	-175.551
Heavy atoms	33	29	33	33	32
H-bonding energy	-11.9416	-9.89572	-10.9408	-10.2336	-9.55797
Torsions No. of rotatable bonds	9	10	10	8	8
Rerank score	-130.24	-112.207	-98.3151	-128.719	-124.596

**Fig. 4** Position of ligand in the cavity 1 of PTA: **a** ZINC08442078, **b** ZINC08442087, **c** ZINC08442182, **d** ZINC08442184 and **e** ZINC08442200

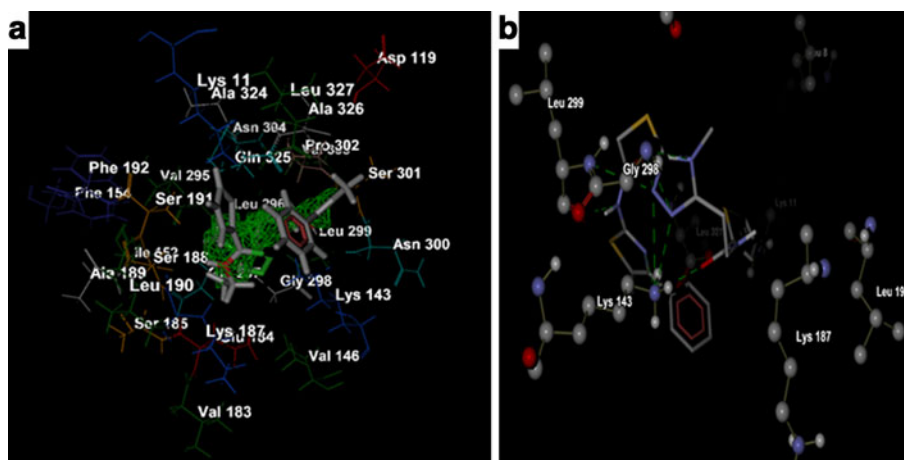


Fig. 5 The residues involved in the formation cavity 1 (a) and residues involved in hydrogen bond, i.e., Leu299, Gly298 and Lys143 (b)

pharmacological properties, the Toxtree, a full-featured and flexible user-friendly open source application, was used to estimate the toxic hazardous properties. User-defined molecular structures are also supported—they could be entered by SMILES or using the built-in 2D structure diagram editor [19]. The other properties like absorption distribution, metabolism and excretion (ADME) were also predicted. Finally, five molecules have been selected, based on the above properties (Table 2).

Due to the evolving technologies in the area of bioinformatics and combinatorial chemistry, the number of known targets as well as the size of compound libraries available is exploding. It has been evaluated that these five molecules were non-carcinogenic, and virtual screening using pharmacophore has proved to be a major technique for pre-screening compounds from libraries against targets *in silico* [19, 50]. A pharmacophore is defined as an ensemble of universal chemical features that characterise a specific mode of action of a ligand in the active site of the macromolecule in 3D space. Chemical features are, e.g. hydrogen bonds, charge interaction, hydrophobic areas, etc. after finding the top 5 ligands (drug-like molecule) from virtual screening of ligand library; we have done structural alignment of these molecules using the ZINC08442078 as a reference molecule in the Ligandscout 2.03 software (it is a software tool that allows to rapidly and transparently derive 3D pharmacophores from structural data of macromolecule/ligand complexes in a fully automated and convenient way) and generated the hypothetical pharmacophore model for phosphotransacetylase. The shared feature pharmacophore model shows only six feature pharmacophores, one of which is a yellow sphere, i.e. hydrophobic feature, one hydrogen bond donor (green vectors), one aromatic ring and three hydrogen bond acceptor, while the merged feature pharmacophore shows eight hydrophobic feature, four hydrogen bond donor, nine aromatic ring and 11 hydrogen bond acceptor. The alignment of five ligands, shared pharmacophore model, shared pharmacophore model as well as merged pharmacophore model is shown in the following Fig. 6. Overall, we selected the PTA as a putative target, and for *S. aureus*, the insights of this enzyme revealed were by some computational methods using standard algorithms. By this study, we had tried to uncover the putative interaction of enzyme and ligand. This study will be helpful for the design and selection of antimicrobials and respective adjuvants for appropriate action.

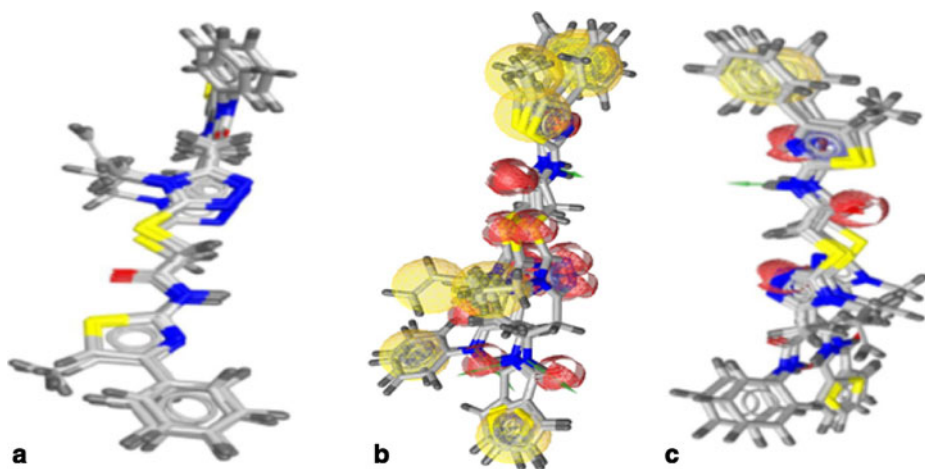


Fig. 6 Pharmacophore mapping of the ligand, ZINC08442078, ZINC08442087, ZINC08442182, ZINC08442184 and ZINC08442200. **a** The alignment of selected ligands. **b** Shared feature pharmacophore. **c** Merged feature pharmacophore

There are several examples showing successful inhibitor development using virtual screening approaches. The first successful experimental test of docking was carried out using the DOCK programme to search a diverse subset of molecules that might bind to HIV-1 protease [54–57]. One of the ligands from the VS was bromoperidol, a close analog of which haloperidol was tested and found to be an HIV-protease inhibitor, and subsequent analog synthesis yielded a thioetheral derivative with 15 μM inhibition. Furthermore, Merck's HIV protease inhibitor Indinavir sulphate was developed in part using docking [58].

Anyhow these admonitions, virtual screening is a perpetually very important tool for exploring biologically relevant chemical space. Thus, a larger virtual screening study focused on small molecules libraries, up to millions of compound. In our previous work, we have analysed the metabolic pathways in the finding of essential protein, which could be targeted for drug designing. A comparative study of the metabolome of *S. aureus* bestows the idea that essential enzymes can be targeted for the drug designing [5], and eight imperative proteins were identified from the organism. Out of these putative targets, PTA was selected for present work, as it was found to be a non-homologous protein in comparison with human protein, thus could be a safer target. The reported molecule as inhibitor to this enzyme could further be exploited for drug design. Here, we described a comprehensive and efficient molecular modelling and docking methodology, which is able to explore the active site and the binding of inhibitor. It is still needed to explore some more in vivo experimentation for complete evaluation as a drug. Using this selectable approach for designing the drug, a researcher can minimise the try and hit methodology; thus, it can save the time, cost and life of test animals. Furthermore, the present study reveals that some molecules with putative drug-like properties could be explored as antimicrobial against *S. aureus*.

Acknowledgments This study was supported by a grant of the Korea Healthcare Technology R&D Project, Ministry of Health & Welfare, Republic of Korea (grant no. A103017). The work was also supported in part by Inha University.

References

1. Carleton, H. A., Diep, B. A., Charlebois, E. D., Sensabaugh, G. F., & Perdreau-Remington, F. (2004). Community-adapted methicillin-resistant *Staphylococcus aureus* (MRSA): population dynamics of an expanding community reservoir of MRSA. *Journal of Infectious Diseases*, *190*, 1730–1738.
2. Diekema, D. J., Pfaller, M. A., & Schmitz, F. J. (2001). Survey of infections due to *Staphylococcus* species: frequency of occurrence and antimicrobial susceptibility of isolates collected in the SENTRY Antimicrobial Surveillance Program. *Clinical Infectious Diseases*, *32*, S114–S132.
3. Freeman-cook, L., & Freeman-cook, K. (2006). *Staphylococcus aureus* infections (deadly diseases and epidemics). Philadelphia, Chelsea House Publications.
4. King, M. D., Humphrey, B. J., Wang, Y. F., Kourbatova, E. V., Ray, S. M., & Blumberg, H. M. (2006). Emergence of community-acquired methicillin-resistant *Staphylococcus aureus* USA 300 clone as the predominant cause of skin and soft-tissue infections. *Annals of Internal Medicine*, *144*, 309–317.
5. Morya, V. K., Dewaker, V., Mecarty, S. D., & Singh, R. (2010). In silico analysis metabolic pathways for identification of putative drug targets for *Staphylococcus aureus*. *Journal of Computer Science & Systems Biology*, *3*(3), 062–069.
6. Ross, R. A., & Onderdonk, A. B. (2000). Production of toxic shock syndrome toxin 1 by *Staphylococcus aureus* requires both oxygen and carbon dioxide. *Infection and Immunity*, *68*(9), 5205–5209.
7. Yarwood, J. M., & Schlievert, P. M. (2003). Quorum sensing in *Staphylococcus* infections. *The Journal of Clinical Investigation*, *112*(11), 1620–1625.
8. Bien, J., Sokolova, O., & Bozko, P. (2011). Characterization of virulence factors of *Staphylococcus aureus*: novel function of known virulence factors that are implicated in activation of airway epithelial proinflammatory response. *Journal of Pathogens*, *2011*(601905), 13. doi:10.4061/2011/601905.
9. Deurenberg, R. H., & Stobberingh, E. E. (2008). The evolution of *Staphylococcus aureus*. *Infection, Genetics and Evolution*, *8*(6), 747–763.
10. Ellis, M. W., Griffith, M. E., Jorgensen, J. H., Hospenthal, D. R., Mende, K., & Patterson, J. E. (2009). Presence and molecular epidemiology of virulence factors in methicillin-resistant *Staphylococcus aureus*-strains colonizing and infecting soldiers. *Journal of Clinical Microbiology*, *47*(4), 940–945.
11. Ferry, T., Perpoint, T., Vandenesch, F., & Etienne, J. (2005). Virulence determinants in *Staphylococcus aureus* and their involvement in clinical syndromes. *Current Infectious Disease Reports*, *7*, 420–428.
12. Hogeveik, H., Söderquist, B., Tung, H. S., Olaison, L., Westberg, A., Rydén, C., Tarkowski, A., & Andersson, R. (1998). Virulence factors of *Staphylococcus aureus* strains causing infective endocarditis—a comparison with strains from skin infections. *APMIS*, *106*(9), 901–908.
13. Spanu, V., Spanu, C., Virdis, S., Cossu, F., Scarano, C., & De Santis, E. P. (2012). Virulence factors and genetic variability of *Staphylococcus aureus* strains isolated from raw sheep's milk cheese. *International Journal of Food Microbiology*, *153*(1–2), 53–57.
14. Lowy, F. D. (1998). *Staphylococcus aureus* infections. *The New England Journal of Medicine*, *339*, 520–532.
15. Sarkar, M., Maganti, L., Ghoshal, N., & Dutta, C. (2012). In silico quest for putative drug targets in *Helicobacter pylori* HPAG1: molecular modeling of candidate enzymes from lipopolysaccharide biosynthesis pathway. *Journal of Molecular Modelling*, *18*(5), 1855–1866.
16. Perumal, D., Lim, C. S., Sakharkar, K. R., & Sakharkar, M. K. (2007). Differential genome analyses of metabolic enzymes in *Pseudomonas aeruginosa* for drug target identification. *Silico Biology*, *7*(4–5), 453–465.
17. Butt, A. M., Tahir, S., Nasrullah, I., Idrees, M., Lu, J., & Tong, Y. (2012). *Mycoplasma genitalium*: a comparative genomics study of metabolic pathways for the identification of drug and vaccine targets. *Infection, Genetics and Evolution*, *12*(1), 53–62.
18. Morya, V. K., Kumari, S., & Kim, E. (2011). Imperative pathway analysis to identify the potential drug target for *Aspergillus* infection. *International Journal of Latest Trends in Computing*, *2*(1), 178–182.
19. Morya, V. K., Kumari, S., & Kim, E. K. (2012). Virtual screening and evaluation of ketol-acid reductoisomerase (KARI) as a putative drug target for aspergillosis. *Clinical Proteomics*, *9*(1), 1.
20. Dutta, A., Singh, S. K., Ghosh, P., Mukherjee, R., Mitter, S., & Bandyopadhyay, D. (2006). In silico identification of potential therapeutic targets in the human pathogen *Helicobacter pylori*. *Silico Biology*, *6* (1–2), 43–47.
21. Singh, S., Joshi, P., & Chopade, B. A. (2011). Pathway analysis of *Acinetobacter baylyi*: a combined bioinformatic and genomics approach. *Chemical Biology & Drug Design*, *78*(5), 893–905. doi:10.1111/j.1747-0285.2011.01191.x.
22. Bologna, F. P., Campos-Bermudez, V. A., Saavedra, D. D., Andreo, C. S., & Drincovich, M. F. (2010). Characterization of *Escherichia coli* EutD: a phosphotransacetylase of the ethanolamine operon. *Journal of Microbiology*, *48*(5), 629–636.

23. Campos-Bermudez, V. A., Bologna, F. P., Andreo, C. S., & Drincovich, M. F. (2010). Functional dissection of *Escherichia coli* phosphotransacetylase structural domains and analysis of key compounds involved in activity regulation. *FEBS Journal*, 277(8), 1957–1966.
24. Dimou, M., Venieraki, A., Liakopoulos, G., & Katinakis, P. (2011). Cloning, characterization and transcriptional analysis of two phosphate acetyltransferase isoforms from *Azotobacter vinelandii*. *Molecular Biology Reports*, 38(6), 3653–3663.
25. Xu, Q. S., Jancarik, J., Lou, Y., Kuznetsova, K., Yakunin, A. F., Yokota, H., Adams, P., Kim, R., & Kim, S. H. (2005). Crystal structures of a phosphotransacetylase from *Bacillus subtilis* and its complex with acetyl phosphate. *Journal of Structural and Functional Genomics*, 6(4), 269–279.
26. Iyer, P. P., Lawrence, S. H., Luther, K. B., Rajashankar, K. R., Yennawar, H. P., Ferry, J. G., & Schindelin, H. (2004). Crystal structure of phosphotransacetylase from the methanogenic archaeon *Methanosarcina thermophila*. *Structure*, 12(4), 559–567.
27. Rasche, M. E., Smith, K. S., & Ferry, G. J. (1997). Identification of cysteine and arginine residues essential for the phosphotransacetylase from *Methanosarcina thermophila*. *Journal of Bacteriology*, 179(24), 7712–7717.
28. Gill, S. C., & Von Hippel, P. H. (1989). Extinction coefficient. *Analytical Biochemistry*, 182, 319–328.
29. Guruprasad, K., Reddy, B. V. P., & Pandit, M. W. (1990). Correlation between stability of a protein and its dipeptide composition: a novel approach for predicting in vivo stability of a protein from its primary sequence. *Protection Engineering*, 4, 155–164.
30. Ikai, A. J. (1980). Thermo stability and aliphatic index of globular proteins. *Journal of Biochemistry*, 88, 1895–1898.
31. Kyte, J., & Doolittle, R. F. (1982). A simple method for displaying the hydropathic character of a protein. *Journal of Molecular Biology*, 157, 105–132.
32. Gasteiger, E. (2005). Protein identification and analysis tools on the ExpASY Server. In: J. M. Walker (Ed.), *The proteomics protocols handbook* (pp. 571–607). Totowa: Humana.
33. Geourjon, C., & Deléage, G. (1995). SOPMA: significant improvements in protein secondary structure prediction by consensus prediction from multiple alignments. *Computer Applications in the Biosciences*, 11, 681–684.
34. Lu, Z., Szafron, D., Greiner, R., Lu, P., Wishart, D. S., Poulin, B., Anvik, J., Macdonell, C., & Eisner, R. (2004). Predicting subcellular localization of proteins using machine-learned classifiers. *Bioinformatics*, 20(4), 547–556.
35. Falquet, L., Pagni, M., Bucher, P., Hulo, N., Sigrist, C. J., Hofmann, K., & Bairoch, A. (2002). The PROSITE database, its status in 2002. *Nucleic Acids Research*, 30(1), 235–238.
36. Lambert, C., Léonard, N., De Bolle, X., & Depiereux, E. (2002). ESyPred3D: prediction of proteins 3D structures. *Bioinformatics*, 18(9), 1250–1256.
37. Heinig, M., & Frishman, D. (2004). STRIDE: a web server for secondary structure assignment from known atomic coordinates of protein. *Nucleic Acids Research*, 32, W500–W502.
38. Krieger, E., Joo, K., Lee, J., Lee, J., Raman, S., Thompson, J., Tyka, M., Baker, D., & Karplus, K. (2009). Improving physical realism, stereochemistry, and side-chain accuracy in homology modeling: four approaches that performed well in CASP8. *Proteins*, 77(Suppl 9), 114–122.
39. Maiti, R., Gary, H., Domselaar, V., Zhang, H., & Wishart, D. S. (2004). SuperPose: a simple server for sophisticated structural superposition. *Nucleic Acids Research*, 32, W590–W594.
40. Laskowski, R. A., MacArthur, M. W., Moss, D. S., & Thornton, J. M. (1993). PROCHECK: a program to check the stereochemical quality of protein structures. *Journal of Applied Crystallography*, 26, 283–291.
41. Porter, C. T., Bartlett, G. J., & Thornton, J. M. (2004). The Catalytic Site Atlas: a resource of catalytic sites and residues identified in enzymes using structural data. *Nucleic Acids Research*, 32, D129–D133.
42. Irwin, J. J., & Shoichet, B. K. (2005). ZINC—a free database of commercially available compounds for virtual screening. *Journal of Chemical Information and Modeling*, 45(1), 177–182.
43. Thomsen, R., & Christensen, M. H. (2006). MolDock: a new technique for high-accuracy molecular docking. *Journal of Medicinal Chemistry*, 49(11), 3315–3321.
44. Wolber, G., & Langer, T. (2005). LigandScout: 3-D pharmacophores derived from protein-bound ligands and their use as virtual screening filters. *Journal of Chemical Information and Modeling*, 45(1), 160–169.
45. Wolber, G., Seidel, T., Bendix, F., & Langer, T. (2008). Molecule-pharmacophore superpositioning and pattern matching in computational drug design. *Drug Discovery Today*, 13(1–2), 23–29.
46. Lawrence, S. H., Luther, K. B., Schindelin, H., & Ferry, J. G. (2006). Structural and functional studies suggest a catalytic mechanism for the phosphotransacetylase from *Methanosarcina thermophila*. *Journal of Bacteriology*, 188(3), 1143–1154.
47. Lee, M. R., Tsai, J., Baker, D., & Kollman, P. A. (2001). Molecular dynamics in the endgame of protein structure prediction. *Journal of Molecular Biology*, 313, 417–430.
48. Engh, R. A., & Huber, R. (1991). Accurate bond and angle parameters for X-ray protein structure refinement. *Acta Crystallographica*, A47, 392–400.
49. Vianna, C. P., & de Azevedo, W. F., Jr. (2012). Identification of new potential *Mycobacterium tuberculosis* shikimate kinase inhibitors through molecular docking simulations. *Journal of Molecular Modelling*, 18(2), 755–764.

50. Wermuth, C., & Langer, T. (1998). In H. Kubinyi (Ed.), *Pharmacophore Identification* (pp. 117–136). Leiden: Escom.
51. Lipinski, C. A., Lombardo, F., Dominy, B. W., & Feeney, P. J. (1997). Experimental and computational approaches to estimate solubility and permeability in drug discovery and development settings. *Advanced Drug Delivery Reviews*, 23, 3–25.
52. Lipinski, C. A., Lombardo, F., Dominy, B. W., & Feeney, P. J. (2001). Experimental and computational approaches to estimate solubility and permeability in drug discovery and development settings. *Advanced Drug Delivery Reviews*, 46(1–3), 3–26.
53. Morya, V. K., Yadav, S., Kim, E. K., & Yadav, D. (2012). In silico characterization of alkaline proteases from different species of *Aspergillus*. *Applied Biochemistry and Biotechnology*, 166(1), 243–257.
54. Moraes, F. P., & de Azevedo, W. F., Jr. (2012). Targeting imidazoline site on monoamine oxidase B through molecular docking simulations. *Journal of Molecular Modelling*, 18, 3877–3886. doi:10.1007/s00894-012-1390-7.
55. Heberlé, G., & De Azevedo, W. F., Jr. (2011). Bio-inspired algorithms applied to molecular docking simulations. *Current Medicinal Chemistry*, 18(9), 1339–1352.
56. Dias, R., & de Azevedo, W. F., Jr. (2008). Molecular docking algorithms. *Current Drug Targets*, 9(12), 1040–1047.
57. Kuntz, I. D., Blaney, J. M., Oatley, S. J., Langridge, R., & Ferrin, T. E. (1982). A geometric approach to macromolecule–ligand interactions. *Journal of Molecular Biology*, 161(2), 269–288.
58. DesJarlais, R. L., Seibel, G. L., Kuntz, I. D., Furth, P. S., Alvarez, J. C., Ortiz de Montellano, P. R., De Camp, D. L., Babé, L. M., & Craik, C. S. (1990). Structure-based design of nonpeptide inhibitors specific for the human immunodeficiency virus 1 protease. *Proceedings of the National Academy of Sciences of the United States of America*, 87(17), 6644–6648.